1

Introduction and General Background Concepts

1.1 Why Surfaces?

The growth in the study of solid surfaces and in the number of techniques available for their study has been enormous since the early 1960s. At least one reason for this has been a growing awareness of the importance of understanding surface properties, and indeed the fact that work on surfaces has had an impact on this understanding and on specific applications in the 'real world'. At a fundamental level, surfaces are of great interest because they represent a rather special kind of defect in the solid state; much of our understanding of solids is based on the fact that they are, in essence, perfectly periodic in three dimensions. Indeed, their electronic and vibrational properties can be described in great detail using methods that rely on this periodicity. The introduction of a surface breaks this periodicity in one direction and can lead to structural changes as well as the introduction of localised electronic and vibrational states. Gaining a proper understanding of these effects is not only an academic concern as there is growing interest in the properties of low-dimensional structures in semiconductor devices, and a free surface can represent the simplest case of such a structure.

Perhaps the most widely quoted motivation for modern surface science is the goal of understanding heterogeneous catalysis. The greatly increased rates of certain chemical interactions that occur in the presence of a solid (usually powder) catalyst must result from the modification of at least one of the constituent chemicals adsorbed on the solid surface, which thereby gains an enhanced ability to interact with the other constituent(s) while in this state. One would therefore like to understand what these modifications are, whether there are new intermediate species formed, what are the rate-limiting steps and activation energies, what kind of sites on the catalyst surface are active and how these processes depend on the catalyst material. This might lead to better or cheaper catalysts; at present many such catalysts are based on precious metals such as platinum and palladium.

https://doi.org/10.1017/CBO9781139149716.004 Published online by Cambridge University Press

The problems of understanding these processes in a microscopic or atomistic way are formidable. Industrial processes frequently operate at high temperatures and pressures (i.e. many atmospheres) and the catalysts are in the form of highly dispersed powders, possibly with individual particles comprising only hundreds of atoms. Moreover, they frequently involve transition metals on oxide 'supports' that may or may not be passive, and they may include small additions of 'promoters' that greatly enhance the efficiency of the catalysts.

The scientific approach to addressing these questions, which makes the fullest use of the techniques described in this book, is to study highly simplified versions of these problems. This involves initially taking flat, usually low-Miller-index, faces of single crystals of the material of interest and studying the adsorption or coadsorption of small quantities of atoms and molecules on them in an otherwise ultra-high-vacuum (UHV) environment. The objective of this approach is to characterise the surfaces and the associated adsorption and reaction processes in fine detail so that the conditions are very well defined. It is easy to see reasons why this approach may be too far removed from applied catalytic problems to be of real value, yet even in the early 1980s some understanding of simple catalytic reactions at a microscopic level had started to emerge from these model studies (King & Woodruff, 1982). Since then, problems of increasing complexity have been explored with significant success, although there is also growing interest in trying to extend some methods to higher 'near-ambient' pressures. The objective here is to bridge the 'pressure gap' that exists in those cases in which the fundamental processes at low and high pressure have been found to differ.

Another area of interest in surface science is to understand the corrosion of materials and certain kinds of mechanical failure due to grain boundary embrittlement. One important process in these problems is of the segregation of minority ingredients (often impurities) in a solid to the free surface, or to internal surfaces (grain boundaries), when the temperature is high enough to allow diffusion through the bulk at a reasonable rate. Some specific species can find it very energetically favourable to be in one of these surface sites rather than in the bulk, so that a bulk concentration of even a few parts per million can lead to surfaces or interfaces covered with a complete atomic layer of the segregant in equilibrium. Segregation of this kind is now well established as being a cause of intergranular fracture of engineering materials. On the other hand, similar segregation to free surfaces can have the effect of improving resistance to corrosion. Studies in this broadly metallurgical area have proceeded not only by the simplified model investigations described above but also by applying surface science techniques to investigate the surfaces of 'real' materials of interest. In particular, by determining the composition of the top few atomic layers of a fractured or corroded surface, considerable information can be gained. To do this, one requires techniques which are highly surface specific in their

analytic capabilities. Coupled with a method of removing atomic layers in a reasonably controlled fashion, usually by ion bombardment, a depth profile of the surface and subsurface composition can be obtained.

A further area of application of surface studies that lies particularly close to the fundamental problems mentioned at the beginning of this section concerns the fabrication of semiconductor devices. Although there are applications for depth profiling on actual devices for the 'troubleshooting' of production problems (due to contamination or interdiffusion at interfaces), there are also problems of quite fundamental importance which lie naturally quite close to the modelling approach used in catalytically motivated research. For example, the formation of metal–semiconductor junctions with desirable properties is strongly influenced by the tendency for chemical interactions to occur between the metal and the semiconductor. Many real devices are based on well-oriented single-crystal materials, so this aspect of the modelling is no longer idealised. Moreover, in the case of semiconductor surfaces some of the simplest problems remain far from trivial to solve. Most semiconductor surfaces appear to involve some structural rearrangement of the atoms relative to a simple extension of the bulk structure. For example, the stable structure of a clean Si{111} surface reconstructs to a 'superlattice' seven times larger in periodicity than the bulk (this superlattice is a (7×7) structure in the notation described in section 1.7). A proper quantitative understanding of this complex reconstruction proved to be one of the key problems of basic surface science in the early years, but by the late 1980s a rather clear picture had emerged by the use of a combination of methods (of which high energy electron diffraction, a method not normally used in surface studies, and scanning tunnelling microscopy (STM) played a key role). Simpler reconstructions also occur at some semiconductor surfaces. Even in the case of the {110} cleavage faces of III–V compounds such as GaAs, at which there is no change in the two-dimensional periodicity of the surface, there is a rearrangement in bond angles influencing the relative positions of the Ga and As layers. Finally, it is notable that there is continuing interest in the growth of semiconductor devices by methods such as molecular beam epitaxy (MBE) that are similar to those used in surface science generally (UHV and 'adsorption' at very low rates). The surface structures formed during MBE can be very complex and highly sensitive to the stoichiometry of the uppermost layer. Growth studies also reveal that many materials will not grow in a layer-by-layer form on certain other layers. These limitations in 'atomic engineering' need to be understood properly if exotic multilayer devices are to be designed and built.

The development of atomic-scale imaging methods of surfaces as part of the surface science armoury has also led to an increasing impact in the study of nanoscience and nanomaterials. The properties of solids and surfaces on the nanometre scale (as in traditional heterogeneous catalysts but also increasingly in modern

nano-engineered materials) are often fundamentally different from those of extended solids, owing to the dominance of the surface and to quantum size effects.

This book is concerned with the analytical techniques which have contributed, and should continue to contribute, to understanding these problems. It is concerned with the basic underlying physical principles of the techniques and the extent to which those principles constrain their usefulness. As such, it is not intended to be an experimental handbook for surface analysis but rather to provide the background of physical understanding that allows the techniques to be used and assessed properly. Some experimental details are given, but only to aid in understanding the strengths and limitations of individual techniques. During almost 50 years in the development of modern surface science a large number of novel methods have been explored; the focus here is on those techniques that continue to play a significant role in surface studies.

A few preliminary comments are in order regarding units. In general, SI units are adopted in this book; hence the decision in this edition to express vacuum pressures in mbar rather than torr as a unit of pressure (see section 1.3). However, this adherence to SI units will be allowed to lapse in the expression of lengths to more intuitive or convenient units. Typical samples have dimensions of ~1 cm^2, so surface coverages will be expressed in terms of a number per cm^2 rather than per m^2, while interatomic spacings and layer spacings will be expressed in ångströms, arguably a more natural unit than the nearest SI unit, nanometres (1 Å = 0.1 nm).

1.2 Ultra-High Vacuum (UHV), Contamination and Cleaning

If one is to study the properties of a surface that are well characterised at an atomic level it is clear that the composition of the surface must remain essentially constant over the duration of a measurement. In order to achieve this, the rate of arrival of reactive species from the surrounding gas phase must be low. A reasonable criterion would be that no more than a few per cent of an atomic layer of atoms should attach themselves to the surface from the gas phase in, say, an experimental time scale of about one hour. This requirement can be evaluated readily from the simple kinetic theory of gases. Thus, the rate of arrival of atoms or molecules from a gas of number density n per unit volume and with an average velocity c_a is

$$r = \frac{1}{4} n c_a \tag{1.1}$$

Equating the kinetic energy of a particle of mass m with root mean square velocity c_{rms} to its thermal energy, determined by the absolute temperature T and Boltzmann's constant k_B, gives

https://doi.org/10.1017/CBO9781139149716.004 Published online by Cambridge University Press

$$c_{\mathrm{rms}}^2 = 3k_{\mathrm{B}}T/m \tag{1.2}$$

Combining the relationship between the two velocities,

$$c_{\mathrm{a}} = (8/3\pi)^{1/2} c_{\mathrm{rms}} \tag{1.3}$$

with the fact that the pressure P is given by

$$P = nk_{\mathrm{B}}T \tag{1.4}$$

then leads to an expression for the rate of arrival:

$$r = P(1/2\pi k_{\mathrm{B}}Tm)^{1/2} \tag{1.5}$$

A convenient form of this expression, in which P is expressed in mbar, T is in K and m is substituted by the molecular weight M multiplied by the atomic mass unit, gives

$$r = 2.66 \times 10^{22} P/(TM)^{1/2} \tag{1.6}$$

with r in molecules cm^{-2} s^{-1}. For example, N_2 molecules (M = 28) at room temperature (T = 293 K) in a pressure of 1 mbar have an arrival rate of 2.95×10^{20} molecules cm^{-2} s^{-1}.

It is convenient to define a *monolayer* adsorption time in terms of the pressure. In defining this it is assumed that a monolayer, i.e. a single complete atomic layer, consists of about $(1-2) \times 10^{15}$ atoms cm^{-2} and that all molecules arriving at the surface stick and are incorporated into this monolayer. Thus, for this example, the monolayer time is about 4×10^{-6} s at 1 mbar, 4 s at 10^{-6} mbar and more than 1 hour at 10^{-9} mbar. This means that if all the gas atoms and molecules arriving at a surface in a vacuum system do indeed stick to it, then the contamination of a few per cent of a monolayer in an experimental time of 1 hour requires a low pressure of 10^{-10} mbar or better. While these are broadly worst-case assumptions, some surfaces of interest do react readily with H_2 and CO, the main ingredients of a UHV chamber, and so match these conditions. An ultra-high vacuum is therefore required to keep a surface in its clean or otherwise well-characterised condition once produced. Indeed, the need for a good vacuum can also extend to the kind of depth profiling study of technical surfaces described in the previous section. In these cases a sample is initially analysed 'as loaded' so that the surface composition is dominated by contamination from being handled in air and is uninfluenced by the quality of the surrounding vacuum in the analysis chamber. However, once surface layers have been removed in the depth profiling, the freshly exposed surface is susceptible to new contamination and must be studied in a good-quality vacuum.

A detailed discussion of the methods for achieving UHV is not appropriate to this book and can be found in many volumes concerned specifically with vacuum technology (e.g. Delchar, 1993; Chambers *et al.*, 1998; Chambers, 2005). A few points of general interest are worth noting, however. The first is that a major reason for the development of modern surface science research in the 1960s, in addition to those given in the previous section, is the commercial availability of convenient UHV components since that time and their subsequent development. Early surface science experiments were carried out in glass vacuum systems using liquid N_2 trapped Hg diffusion pumps. The surface science instrumentation had to be incorporated into these sealed glass vessels with electrical connections made through glass-to-metal seals in the containment vessel. Modern surface science studies usually involve the use of many different techniques in the same vessel, each of which may be quite sophisticated, and this is achieved by mounting each onto a stainless steel flange sealed to a stainless steel chamber using Cu gaskets or Au wire seals. This gives great flexibility and demountability for installation, modification and maintenance; it is hard to see how the current level of sophistication of some surface science experiments could have been achieved realistically with glass systems. In addition to the development of these demountable metal vessels, great use is now made of ion pumps and turbomolecular pumps, which require only electrical power to function and do not need liquid N_2 cooling and the regular attention that this implies.

The second general point regarding UHV is the constraints on fabrication methods necessary for instrumentation within the vacuum. Although one must use vacuum pumps capable of operating in the 10^{-10}–10^{-11} mbar range, an important ingredient in obtaining UHV is the need to 'bake' the whole system. In the absence of leaks and with suitable pumps, vacua are limited by the 'outgassing' of the inner walls and instrument surfaces within the chamber, mainly due to the desorption of weakly adsorbed gases from these surfaces. By heating all these surfaces the rate of desorption is increased and the surface coverage decreased, and thus the rate of desorption on the subsequent cooling to room temperature is reduced. This reduces the gas load on the pumps and thus allows lower pressures to be achieved. Typically, a stainless steel chamber with all its enclosed instrumentation is baked at temperatures of ~140–200 °C for 12–24 hours. Obviously this means that all components in the vacuum chamber must be stable and have low vapour pressures at these elevated temperatures. An additional common requirement for the experiments described in this book is that all components must be non-magnetic as many surface techniques involve low energy electrons, which are easily deflected by weak electrostatic and magnetic fields. Fabrication methods compatible with these requirements are now well established, involving mainly the use of non-magnetic stainless steel and refractory

metals, together with ceramics for electrical or thermal insulation. Many materials that are acceptable in a 'high vacuum' (~10^{-6} mbar), such as some adhesives and plastics, are not acceptable in UHV.

While UHV guarantees that a surface should not be influenced by the arrival of ambient atoms and molecules from the residual gas phase on a time scale of the order of one hour or more, a further requirement for studies of the properties of ideal surfaces is to be able to clean them, in the vacuum system, to a level compatible with the same contamination constraints as those that define the required vacuum; i.e. one must produce a surface which contains no more than a few per cent (and preferably less) of an atomic layer of species other than those that comprise the underlying bulk solid. Generally, the surface should also be well ordered on an atomic scale. The main methods used to achieve this *in situ* cleaning are

(i) cleavage,
(ii) heating,
(iii) ion bombardment,
(iv) chemical processing.

The first of these is largely self-explanatory; for those materials which do cleave readily (e.g. oxides, alkali halides, semiconductors, layer compounds), and for studies of the surface orientation which comprises the cleavage face, surfaces can be prepared in vacuum that are intrinsically clean. Apart from the limitations on the materials and orientations that can be prepared in this way, a significant problem with the method is that it is usually only possible to cleave a single sample (even a long bar) a few times, so the surface cannot be re-prepared many times. It is also possible that cleavage may result in a heavily stepped surface. As a result, large variations in the properties of a surface (particularly the adsorption kinetics) may be obtained from one cleave to the next on many materials. Moreover, on some materials the cleavage surface is found to have a different structure from that obtained by heating to allow the surface to equilibrate; the Si{111} surface is an example of this.

Heating a surface, like heating the walls of a vacuum vessel, can lead to the desorption of adsorbed species. However, in most cases some impurities on the surface are too strongly bound to be removed by heating to temperatures below the melting point of the sample. Heating as a method of cleaning has been used mostly for W and similar high melting point materials, for which the surface oxides are flashed off below the melting point of the underlying metal. Even for these materials, however, it is unlikely that the method can be totally satisfactory owing to impurities such as C, which form exceedingly strongly bound compounds with the substrate material. Once this kind of impurity has been removed, however,

heating alone may be sufficient to regenerate a clean surface following an adsorption experiment using the more weakly bound adsorbate species. This surface regeneration by heating may be applicable to many materials for which heating alone is totally ineffective in the initial cleaning process.

The use of inert-gas (usually Ar) ion bombardment of a surface to remove layers of the surface by sputtering is by far the most widely used primary method, particularly for metal surfaces. The actual physics of this process and the yields obtained are discussed in Chapter 2. The technique is effective in the removal of many atomic layers of a surface and, even if an impurity species is far less effectively sputtered than the substrate, it can generally be removed eventually. One disadvantage of ion bombardment, typically at energies of 0.5−5.0 keV, is that the surface is left in a heavily damaged state, with many atoms statically displaced from their crystalline sites and usually also with embedded Ar atoms; the surface must then be annealed to restore the order. This in itself can create problems; as was noted in the previous section, many dilute impurity species in the bulk of a solid will segregate preferentially to the free surface so if a sample with a clean surface is heated, the diffusion rates are increased and further segregation can occur; typical segregants found in transition metals, even of very high average purity, are C and S. This then requires further ion bombardment cleaning, further annealing and so on. In practice a number of cycles (sometimes as many as ten or more) of bombardment and annealing do lead to the depletion of segregating impurities in the subsurface region and thus to a clean surface. Far fewer cycles are then required for re-cleaning the sample after adsorption studies.

The final approach of chemical cleaning *in situ* involves the introduction of gases into the vacuum system at low pressures (~10^{-6} mbar or less) that react with impurities on a surface to produce weakly bound species, which can then be thermally desorbed. This method is most widely used for the removal of C from refractory metals such as W that can be cleaned of most other impurities by heating alone. Exposure of such a surface to O_2 at elevated temperatures leads to the removal of C as desorbed CO, leaving an oxidised surface that can then be cleaned by heating alone.

1.3 Adsorption at Surfaces

Although several techniques described in this book are applicable to the surface analysis of a wide variety of practical materials problems, the emphasis of the presentation is on applications of the 'surface science method', i.e. studies of well-characterised low index single-crystal surfaces and adsorption of atoms and molecules on them. It is therefore helpful to define some terms and units that will be used in later chapters. The first of these is the definition of a *monolayer* of

adsorbate. One way of defining the coverage of a surface at monolayer level – i.e. of a single complete atomic or molecular layer – is in terms of the coverage of a two-dimensional close-packed layer, taking account of the atomic or molecular size. Such a definition is frequently used in studies of polycrystalline surfaces. However, on surfaces of well-defined crystallography it is generally more convenient to use a definition based on the atomic density of packing in the surface itself. Therefore, unless explicitly stated otherwise, a monolayer of adsorbed atoms or molecules will be defined as a layer having a number density equal to that of the atoms in a single atomic layer of the substrate material parallel to the surface. In the absence of reconstruction, this is, of course, the same as the number density of atoms in the top atomic layer of the substrate. Frequently the saturation of a particular adsorbate species occurs at a coverage of less than one monolayer, so the definition implies nothing about the maximum possible coverage, which depends on the adsorption system under study.

A second definition concerning adsorption studies is the need for a unit of exposure. The unit which had become firmly established in the literature is the langmuir (abbreviated as L), defined as 1 L = 10^{-6} torr s exposure. Unfortunately it is more usual nowadays for pressures to be quoted not in torr (1 torr = 1 mm mercury =1.333 mbar) but in mbar, so 1 L is often (implicitly rather than explicitly) redefined as 10^{-6} mbar s. These two definitions are not, of course, equivalent. Because of this ambiguity, exposures in this book will be given only in units of 10^{-6} mbar s. A major disadvantage of the langmuir unit (and also the unit used here, 10^{-6} mbar s) is that, as may be readily appreciated from equation (1.6), the actual number of atoms or molecules arriving at a surface in 1 L of exposure depends on the molecular weight of the gaseous species and its temperature. Table 1.1 illustrates the effect of this variation, showing the number of molecules striking 1 cm^2 of surface in 1 L with a gas temperature of 300 K. Also shown here is the coverage, in monolayers, which would result if all the molecules arriving were to stick on a Ni{100} surface, with dissociative adsorption assumed for H_2, O_2 and I_2. Despite this disadvantage of the L unit (or its mbar s equivalent), there is no doubt that it is experimentally convenient, as most researchers performing an exposure are equipped with an ion gauge (calibrated in mbar or torr) and a stopwatch! It provides a convenient unit for characterising the exposures needed to produce certain adsorption states on a surface and allows some transferability between experimenters working on the same adsorption system. It also is a unit of convenient magnitude in that, as Table 1.1 shows, 1 L corresponds to approximately one monolayer coverage if all molecules stick to the surface. A proposal for a unit based on the actual number of impinging molecules (Menzel & Fuggle, 1978) failed to gain any long-term support. One further point that is worth mentioning in the context of Table 1.1 is the question of sticking probabilities.

Table 1.1 *Effect of 1 L (10^{-6} torr s) exposure of different adsorbates at 300 K*

Incident and adsorbing species	No. of molecules arriving (cm^{-2})	Coverage on Ni{100} with unit sticking probability (monolayers)
H_2 adsorbing as H	1.43×10^{15}	1.80
O_2 adsorbing as O	3.58×10^{14}	0.44
CO adsorbing as CO	3.83×10^{14}	0.24
I_2 adsorbing as I	1.27×10^{14}	0.16

The final column of Table 1.1 was constructed assuming that all impinging molecules stick to the surface (i.e. that the 'sticking probability' is unity) independent of coverage. In fact this would represent a relatively unusual state of affairs. As the coverage increases, some molecules arriving at the surface will land at sites already occupied by adsorbed species, rather than at vacant clean surface sites. Assuming that these also stick (and then may diffuse over the surface to empty surface sites) actually involves assuming that second layer adsorption (albeit possibly more weakly bound and transient) is possible. An alternative possibility, that the molecules arriving at occupied sites are not adsorbed, leads to an average sticking probability that falls exponentially with time. This *Langmuir adsorption* is one of several possible forms of adsorption kinetics discussed in many books on adsorption (e.g. Hayward & Trapnell, 1964; Masel, 1996; Kolasinski, 2012) and will not be discussed further here. The measurement of sticking probabilities, however, will be considered in Chapter 6. Notice that exposures given in langmuirs (or in 10^{-6} mbar s) that are based on ion gauge readings of total chamber pressures are unlikely to be very reliable for any serious study of adsorption kinetics, owing to difficulties in establishing the pressure at the sample and the need for ion gauge calibration for different gases. For similar reasons, exposures determined in this way using different chambers in different laboratories may lead to variations of a factor 2 or more in the (apparent) exposures needed to obtain particular adsorption states.

Finally, in this book many examples of adsorption systems chosen to illustrate the application of specific techniques may be referred to as involving *chemisorbed* or *physisorbed* atoms or molecules. The distinction between these two types of adsorption lies in the form of the electronic bond between the adsorbate and substrate. If an adsorbed molecule suffers significant electronic modification, relative to its state in the gas phase, to form a chemical bond with the surface (covalent or ionic) then it is said to be chemisorbed. If, however, it is held to the surface only by van der Waals' forces, relying on the polarisability of the otherwise undisturbed molecule, then it is said to be physisorbed. Clearly physisorption

produces weak bonds while chemisorption often produces strong bonds. It is usual to regard the upper limit of the bond strength in physisorption as around 0.6 eV per atom or molecule, or 58 kJ mol^{-1} (1 eV $molecule^{-1}$ = 96.5 kJ mol^{-1} = 23.1 kcal mol^{-1}). Thermal energy considerations (see section 6.3.1) lead to the conclusion that such weakly bonded species would be desorbed from a surface at a temperature much in excess of 200 K. Adsorbates stable on a surface above this sort of temperature are therefore almost certainly chemisorbed. However, the distinction is strictly in terms of the form of the bond, and not its energy, and there are cases in the literature in which electronic modifications characteristic of chemisorption are seen in far more weakly bound species. A low desorption temperature does not, therefore, necessarily indicate physisorption.

1.4 Surface Analytical Techniques, Surface Sensitivity and Surface Specificity

The rest of this book describes the principles and applications of the main techniques used in investigations of the detailed properties of surfaces. In the earlier editions of this book these techniques were organised primarily according to the type of probe used (electrons, ions etc.). This approach was perhaps particularly appropriate during a period when new techniques were frequently being explored and one might ask the question, what can I learn using my electron gun or ion gun? However, specific surface studies are generally motivated by a need to determine the chemical composition of the surface, its structure and morphology, its electronic structure and the molecular identity of species that may be present on the surface. In this edition of the book the techniques have been reorganised according to this classification, allowing more direct comparison of the alternative methods to achieve a defined goal. Of course, either method of organisation necessarily involves quite a lot of cross-referencing.

Any technique that can provide information on the surface of a material – i.e. the outermost few atomic layers – must have two key properties, namely surface sensitivity and surface specificity. The sensitivity requirement arises simply because there is only a very small amount of material in the few atomic layers of interest and within some limited lateral range of the probe used to investigate the surface. For example, a single monolayer contains ~10^{15} atoms cm^{-2}, so if one uses a probe (typically an electron, photon or ion beam) with an area of 1 mm^2 and wishes to detect 1% of a monolayer (an appropriate value to check for impurities), the associated technique must be capable of detecting ~10^{11} atoms, with a corresponding mass, say, for carbon atoms (a typical impurity) of ~10^{-12} g. In many cases the probe area is actually several orders of magnitude smaller than 1 mm^2, so a much higher sensitivity is required. More demanding, however, is the need for surface

specificity: the outermost few layers of atoms that comprise the region of interest are superimposed on underlying bulk material that typically has a thickness of ~1 mm, thus comprising ~4×10^6 atomic layers. The surface layers thus comprise only ~10^{-6} of the total number of layers in the sample. One therefore requires special techniques that detect only the outermost few atomic layers and not the underlying solid. It is these techniques and their applications that are described in this book. Despite the large number of different methods (some are listed in Table 1.2), there are a relatively small number of physical processes that define their surface specificity.

A common theme of many methods involving electron diffraction or electron spectroscopy is that they involve the detection of electrons emitted from the surface having a kinetic energy characteristic of the initial excitation or scattering within the surface. For all these techniques the primary source of surface specificity is inelastic electron scattering. If an electron passes through sufficient layers of the solid to undergo an inelastic scattering event it loses energy and no longer contributes to the detected signal outside the surface, so the degree of surface specificity of the measurement is related to the inelastic scattering mean-free-path; this can be less than 10 Å for low energy ($<$ ~1 keV) electrons. However, elastic scattering also contributes to the surface specificity of these methods. Figure 1.1 shows schematically how this occurs. In the case of electron diffraction, part of the incident flux is scattered out of the surface from each layer, so the incident flux is attenuated as it penetrates into the solid. Of course, elastic scattering is a conservative process so one would not normally expect it to lead to attenuation, but this can occur in the presence of a surface; electrons scattered out of the surface into the vacuum cannot be scattered back into the solid. In the case of low energy electron diffraction (LEED – see Chapter 3), with electron energies ~30–300 eV, the roles of inelastic scattering (on both inward and outward trajectories) and elastic scattering contribute roughly equally to the degree of surface specificity.

The situation is somewhat different for electron spectroscopies such as X-ray photoelectron spectroscopy (XPS) and Auger electron spectroscopy (AES), both described in Chapter 2. In these techniques the electrons to be detected are produced within the surface at a characteristic energy as a result of incident photon or electron excitation. In this case it is only inelastic scattering that can cause attenuation of the detected signal, but the fact that the emitted electrons may undergo elastic scattering events on their travel out of the sample means that the escape path is longer than the direct (unscattered) distance, leading to increased inelastic scattering. Typically these two effects contribute approximately equally to the resulting attenuation length λ, which can be measured experimentally by depositing thin films of known thickness d onto substrates with electron emissions

Table 1.2 *Summary of techniques and their acronyms and abbreviations*

	Composition	Structure and morphology	Electronic structure or chemical state	Molecular character and adsorption
angle-resolved photoelectron spectroscopy (ARPES)			✓	✓
atomic force microscopy (AFM)		✓		✓
Auger electron spectroscopy (AES)	✓		✓	
electron and photon stimulated desorption (ESD, PSD, ESDIAD)	✓	✓		✓
field emission microscopy (FEM)			✓	
field ion microscopy (FIM)		✓		
helium atom scattering (HAS)		✓		
high energy ion scattering (HEIS)	✓	✓		
high-resolution electron energy loss spectroscopy (HREELS)				✓
infrared reflection-absorption spectroscopy (IRAS, RAIRS)				✓
inverse photoemission spectroscopy (IPES)			✓	✓
ion neutralisation spectroscopy (INS)			✓	✓
low energy electron diffraction (LEED)		✓		
low energy electron microscopy (LEEM)		✓		
low energy ion scattering (LEIS)	✓	✓		
medium energy ion scattering (MEIS)	✓	✓		
molecular beam scattering				✓
near-edge X-ray absorption fine structure (NEXAFS)		✓	✓	✓
photoelectron diffraction (PED, XPD, PhD)		✓		
photoelectron and scanning Auger electron microscopy (PEEM & SAM)	✓	✓	✓	
reflection high energy diffraction (RHEED)		✓		

Table 1.2 (*cont.*)

	Composition	Structure and morphology	Electronic structure or chemical state	Molecular character and adsorption
scanning tunnelling microscopy (STM) & spectroscopy (STS)		✓	✓	
secondary ion mass spectrometry (SIMS)	✓			
single crystal adsorption calorimetry (SCAC)				✓
surface extended X-ray absorption fine structure (SEXAFS)		✓		
surface X-ray diffraction (SXRD)		✓		
temperature programmed desorption (TPD)				✓
ultraviolet photoelectron spectroscopy (UPS)			✓	✓
work function determinations			✓	
X-ray photoelectron spectroscopy (XPS)	✓		✓	✓

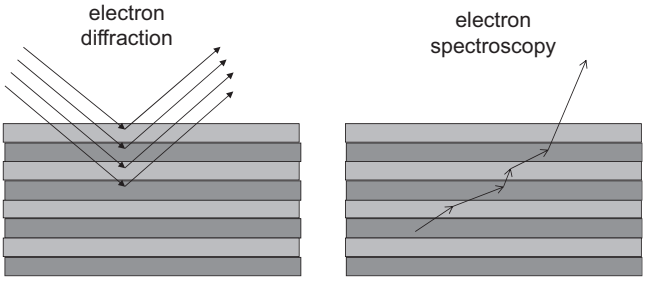

Fig. 1.1 Schematic diagram showing elastic scattering events in electron diffraction and spectroscopy. The atomic layers are represented by shaded slabs.

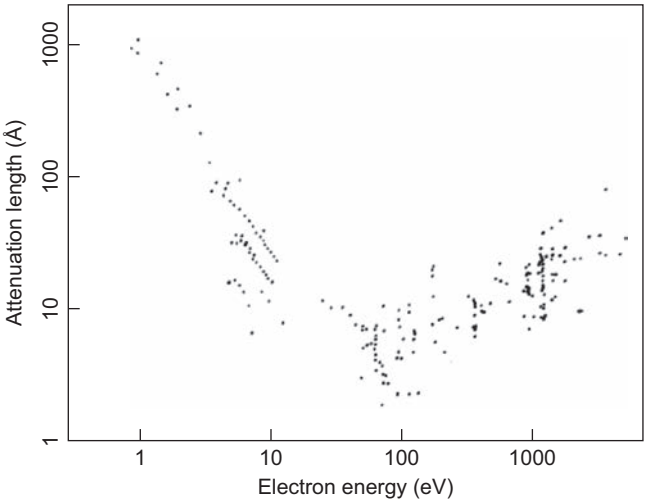

Fig. 1.2 Measured values of the attenuation length due to inelastic scattering as a function of electron energy measured by thin film deposition of a wide range of materials onto substrates with different characteristic electron emission energies. After Seah & Dench (1979). Copyright 1979 Heyden & Son Ltd.

at characteristic energies. The reduction in intensity I relative to the value in the absence of the film, I_0, is given by

$$I = I_0 \exp(-d/\lambda \cos\theta) \tag{1.7}$$

assuming emission at polar angle θ relative to the surface normal. The results of a series of such experiments using different substrate materials and a wide range of atomic and molecular overlayers are shown in Fig. 1.2.

The scatter of the data points in Fig. 1.2 is in part due to the different properties of the range of overlayer materials presented in the graph, but despite this there is a clear general trend of all the data to follow a shape sometimes referred to as the 'universal curve' for electron attenuation. The shape of this curve is closely similar

https://doi.org/10.1017/CBO9781139149716.004 Published online by Cambridge University Press

to that calculated for inelastic scattering alone in an idealised (jellium) model of Al (Quinn, 1962). At the lowest electron energies the attenuation is dominated by single-particle electron–hole excitations, but at higher energies the main contribution comes from the excitation of plasmons – cooperative excitations of the valence electron gas. Plasmon energies are typically in the range 10–30 eV, so there is a steep drop in the attenuation length as this threshold is reached, followed by a slow rise with increasing energy that scales roughly as the square root of the energy. The key result defining the surface specificity of these electron emission techniques is that in a wide energy range, from ~10–1000 eV, the attenuation length is only ~10 Å, or about 3–4 atomic layers. Indeed, in the energy range around ~50–200 eV the attenuation length may reach as low as 5 Å. The detected signal in these emission techniques thus arises from only the outermost few atomic layers.

Notice that photons, be they in the ultraviolet or X-ray range, generally penetrate solids to much greater distances than the few atomic layers that comprise the surface, so a technique such as photoemission, with photons in and electrons out, derives its surface specificity entirely from the scattering of the outgoing electrons. For this reason many techniques based on both photon incidence and photon detection, such as X-ray fluorescence, are not generally surface specific.

Notice that in the case of incident ion techniques, the mechanisms underlying their surface specificity are rather different; the main effect is due to elastic scattering although, for low energy ion scattering, charge exchange neutralisation can also contribute strongly. The 'shadowing' due to elastic scattering is described in sections 2.4 and 3.3, while the influence of charge exchange is described in sections 2.4 and 5.4.

Table 1.2 lists the main techniques discussed in this book, and their abbreviated names, the ticks giving some indication of the kind of information each method can provide. One important generalisation that applies to the study of surfaces is that it is rarely sufficient to use only one technique. At the very least, some limited information in each of three areas, those of geometrical structure, atomic or molecular composition and electronic structure, is needed simultaneously. For this reason most investigations involve several experimental probes on the same chamber, and it is this multi-technique approach which has gained much from the development of stainless steel UHV chambers with demountable flanges in the 1960s. For studies on well-characterised surfaces it was common for many years to include facilities for LEED and Auger electron spectroscopy (AES) or X-ray photoelectron spectroscopy (XPS) in almost all surface science chambers. Low energy electron diffraction provides a simple and convenient characterisation of the surface long range order while AES or XPS provide some indication of chemical composition and, in particular, characterise the cleanness of a surface. The wide use of standard characterisation probes such as LEED and AES has greatly improved our ability to

compare studies of any particular adsorption system by different techniques performed in different laboratories. Of course, the use of these two (or any other) support probes does not totally characterise the surface. A glance at a LEED diffraction pattern shows the basic periodicity of the ordered component of the surface structure but far more study is required to determine the surface structure in detail; i.e. to establish the quality of the order and the relative atomic positions on the surface. There is a good chance, however, that two experimenters both working on the adsorption of some species A on a surface B that produces a particular periodicity of the surface, with a particular maximum level of contamination as seen in AES or XPS, will be working on essentially the same surface. The increasingly widespread use of scanning tunnelling microscopy (STM) provides an alternative (but different) means of characterising the surface order, but the need for a complementary probe of surface composition remains. In comparing different techniques in more detail the special aspects of the individual methods must be considered. One technique may be dominated by the signal from minority species on a surface while another technique probes far more 'averaged' properties. In the chapters that follow these special aspects will be identified and some specific comparisons will be made.

One final remark concerns the application of these techniques to 'technical surfaces'; i.e. to the study of surfaces of polycrystalline materials which have typically undergone some high pressure or wet chemical treatment and are loaded into the vacuum chamber and studied without pre-cleaning. Usually it is of interest to 'depth profile' such surfaces in order to investigate the subsurface as well as the outermost surface. Many of the techniques in Table 1.2 are of little use for these investigations, but a few have proved of great value. In particular, both AES and XPS have been widely used to determine surface and subsurface composition and, particularly with XPS, to identify the chemical state of surface atoms. Low energy ion scattering (LEIS) and secondary ion mass spectrometry (SIMS) have also been used in this way, although SIMS is primarily valued for the analysis of relatively thick films by depth profiling rather than the determination of surface composition. All these techniques are primarily concerned with composition and provide no structural information. Of the techniques listed above, only surface extended X-ray absorption fine structure (SEXAFS) is capable of providing quantitative structural information on a surface independently of whether it is a single crystal (although the structural analysis of individual grains of polycrystalline materials is possible with LEEM).

1.5 Electron, Ion and Photon Probes and Detectors

As remarked above, the focus in this book is on physical principles (rather than experimental details), but there are a few common experimental aspects that are worth highlighting. Many surface techniques involve nominally mono-energetic incident

beams of electrons, ions or photons. In most cases these are produced by standard methods that substantially predate the whole field of surface science. Indeed, in some of the earliest surface studies that required electron beams of a few keV (notably for AES), standard electron guns manufactured for cathode-ray tubes and televisions were used with only a minor modification of the electron source, the fitting of a wire 'hairpin' filament. Simple ion guns exploit very similar electrostatic lenses to those of electron guns for focussing, although the initial source of ions is either the electron ionisation of gas in the high-vacuum pressure range or some kind of discharge or plasma. Most XPS work is performed similarly, using an X-ray source based on the same principle as standard lab-based X-ray diffraction instruments, namely energetic electron impact onto a metal target. The only real difference is that in order to achieve rather lower photon energies (~1.5 keV) than those typically used in X-ray diffraction (~8 keV), lower atomic mass targets (Al and Mg rather than Cu) are used and the X-ray source is built onto the UHV surface science chamber with only a very thin Al window between the source and the sample. In addition, however, one important development in photon sources that has had a significant impact on surface science studies is the use of synchrotron radiation.

Synchrotron radiation is produced when a charged particle (normally an electron) travelling at relativistic speeds is deflected by a magnetic field. In an electron synchrotron or storage ring the electrons are constrained to a nominally circular orbit (strictly speaking, it is a rounded polygon) by a series of bending magnets, and at each such magnet synchrotron radiation is emitted. Classically (at non-relativistic speeds), a circulating electron emits dipole radiation at the circulating frequency, but this is strongly modified by the relativistic effects (for an electron circulating with an energy of 1 GeV, its speed is within $\sim 10^{-7}$ of the velocity of light). In particular, the radiation is very strongly blue-shifted and a very wide range of high harmonics is populated, while the dipolar emission becomes strongly distorted into a narrow cone directed along the instantaneous direction of travel (see Fig. 1.3). The net effect is that this bending magnet radiation is effectively a continuum extending from the far infrared to the hard X-ray range, while the emitted cone of radiation is very narrow ($\sim 1/\gamma$, where γ is the ratio of the total energy and the rest-mass energy of the electron; e.g., for a 1 GeV electron, $\gamma \approx 2000$). As a light source, synchrotron radiation has several exceptional advantages over conventional laboratory sources, namely: (i) essentially all photon energies can be accessed by installing a suitable monochromator, these energies being freely tunable (or more correctly, extractable) by adjustment of the monochromator; (ii) the source has extremely high spectral brilliance (the number of photons per specified bandwidth per unit solid angle), leading to the ability to deliver high photon fluxes to small samples; (iii) the radiation is linearly polarised in the plane of circulation of the electrons. The 'universal curve' for the output flux

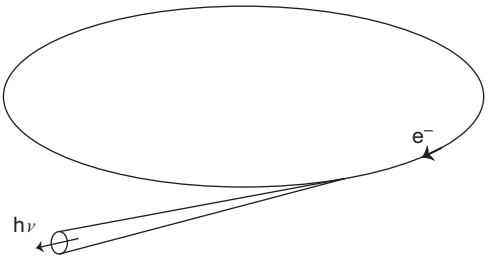

Fig. 1.3 Schematic diagram showing the emission of synchrotron radiation from an electron in a circular orbit at relativistic speeds.

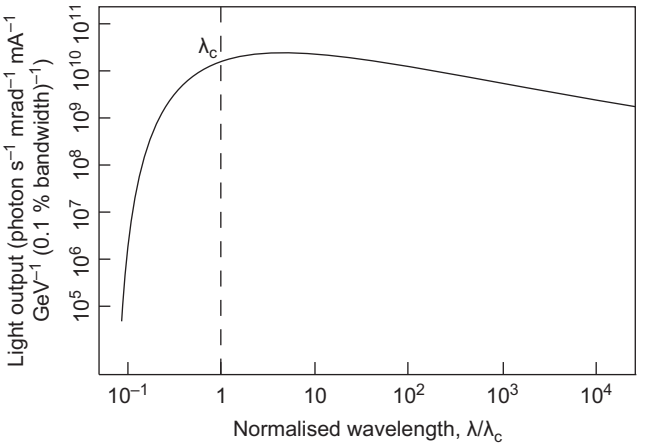

Fig. 1.4 'Universal' spectral curve for synchrotron radiation. The photon flux is normalised to 1 mA of circulating electron current at 1 GeV in the accelerator and is measured in 1 mrad of horizontal divergence. The emitted wavelength λ is normalised to λ_c, which is characteristic of the synchrotron or storage ring. Expressing the electron energy E in GeV and the magnet bending radius R in metres, $\lambda_c = 5.6\ R(E)^{-3}$ in Å. For a typical machine, with E ~3 GeV, λ_c ~1.5 Å so with 300 mA of operating current the peak emission is ~2×10^{13} photons s^{-1} $mrad^{-1}$ (0.1% bandwidth)$^{-1}$.

of bending magnet radiation is shown in Fig. 1.4. However, in modern synchrotron radiation facilities the use of 'insertion devices' – providing arrays of alternating magnetic fields and installed in the straight sections of the storage ring between the bending magnets – can provide even better sources. The simplest of such devices, multipole wigglers, generally have stronger magnetic fields than the bending magnets, leading to more intensity at the highest photon energies; the intensity scales with the number of 'wiggles' experienced by the electrons. However, at somewhat lower fields the radiation from successive 'wiggles' becomes coherent and these undulators deliver radiation concentrated in a small number of harmonics that can be tuned by adjusting the field strength via the gap between the magnet

poles. Moreover, by clever modification of these magnet pole configurations the polarisation can be varied to include circular polarisation as well as different orientations of linear polarisation. More details of the fundamentals of synchrotron radiation and its applications can be found in several texts, such as those by Margaritondo (1988), Duke (2008) and Willmott (2011).

Of course, the disadvantage of synchrotron radiation sources is that they are not available in one's home laboratory, but their advantages for certain experiments are crucial. For example, in structural studies of surfaces by photoelectron diffraction (see section 3.2.1) and X-ray absorption fine structure (see section 3.2.2) the ability to vary the photon energy with controlled polarisation and with high intensity at the sample is essential for the methods. Similarly, in studies of the electronic structure of surfaces using angle-resolved photoemission (section 5.1) these same properties can be crucial.

The second key component of any experiment using an incident electron, ion or photon probe is a means of detecting the species that emerge from the sample as a result of these incident probes, and a common feature of many surface science techniques is the need to detect the number of charged particles (electrons or ions) emitted as a function of their kinetic energy. Much the most common way to achieve this is to use a dispersive analyser based on electrostatic deflection.

The simplest possible electrostatic deflection system would be a pair of parallel plates set at different potentials; this produces a field with parallel and equally spaced planar surfaces of constant potential. If electrons are directed into this field they are deflected, and the greatest deflection over a given length of travel occurs for those of lowest energy; by putting an aperture into one of the plates, electrons in a specific energy range (the width of the range being a function of aperture size and field strength) will emerge. However, if, for example, the electrons are injected into the field nominally perpendicular to the field but with an angular spread about this mean direction, electrons of the same energy will be deflected by different amounts depending on the angle of injection. This means that the signal passing through the aperture will display an energy spread which is degraded by the angular spread of the incident electrons (see Fig. 1.5(a)). As a result, both the energy resolution and transmission of the analyser are degraded by the angular spread of the source. Evidently, a good analyser design should be capable of focussing electrons of the same energy but different angles of injection at the exit aperture. In the parallel plate analyser this can be achieved by injecting the electrons at a suitable angle. Figure 1.5(b) contrasts this focussing domain with the simple conditions just discussed. In Fig. 1.5(b) focussing is achieved by choosing a mean injection angle such that electrons that enter at a steeper angle, and so need a greater deflection to reach the exit aperture, have a larger distance of travel in the region of the deflecting field. Evidently this condition is only well

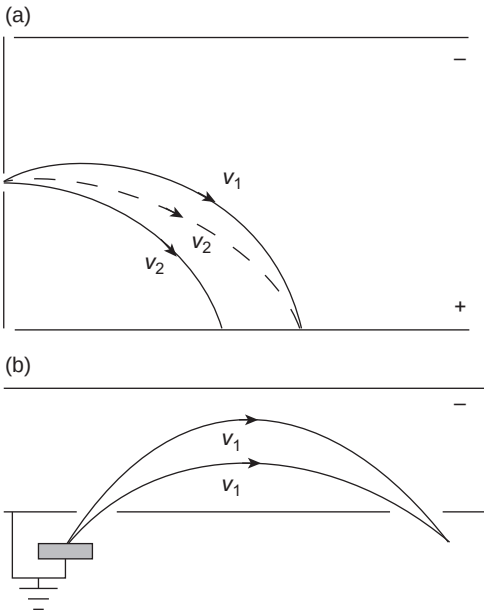

Fig. 1.5 Schematic diagram of electron trajectories in a parallel plate capacitor. In (a) the injection of electrons is approximately perpendicular to the electron field. Electrons with velocity $v_2 > v_1$ are less readily deflected. However, electrons of initial velocity v_1 may arrive at the same point as the axially injected electrons of velocity v_2 if they have the necessary off-axis injection direction; (b) shows a plane mirror analyser (PMA) in a focussing configuration.

satisfied at certain special conditions, and perfect focussing is never obtained. Ideally, a focus position should be independent of the angle of injection relative to the mean direction. In practice one can write an expression for the image position as a polynomial in powers of the divergence angle α (or, in two dimensions, α and β). Geometrical conditions are chosen such that the lowest-order terms vanish, and we then say that we have nth-order focussing if the lowest remaining power of α or β in the expression has order $n + 1$. The remaining, higher-order, terms are referred to as aberrations of the instrument. While the coefficients in this equation are needed to make proper comparison, it is clear that an instrument with second-order focussing is likely to be able to operate usefully with a more divergent source than one having first-order focussing.

Figure 1.6 shows two of the most commonly used types of analyser for surface electron spectroscopies, namely the cylindrical mirror analyser (CMA) and the concentric hemispherical analyser (CHA). The CMA consists of concentric cylinders and accepts a conical annulus about a mean angle from the axis of the analyser of approximately 42°, with second-order focussing. The CHA has a total mean deflection of 180° and first-order focussing.

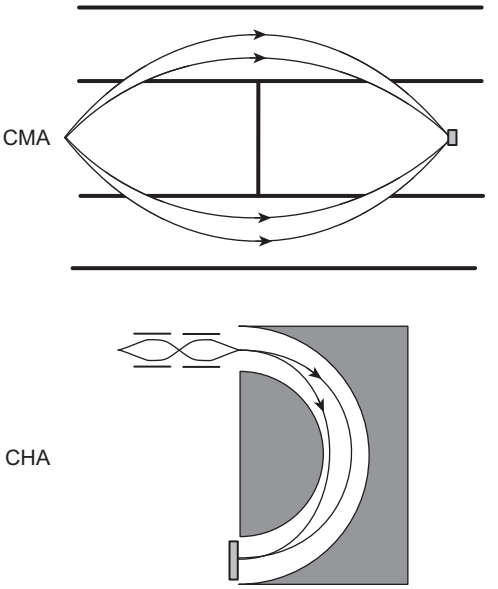

Fig. 1.6 Schematic diagram of analyser geometry and electron trajectories for the CMA and CHA. The CMA has cylindrical symmetry about its axis. The CHA has 180° spherical sector electrodes.

The two main parameters of interest in designing or selecting an analyser for a particular application are the energy resolution and the acceptance angle; both of these also control the sensitivity of the instrument. The energy resolution scales with their physical size. If we define a resolving power as $E_0/\Delta E$ then, excluding aberration terms, the resolving power of these instruments is given by the ratio of a physical dimension related to the total electron pathlength in the analyser and the size of the defining aperture. Thus, for the CHA, this is $2R_0/s$ where R_0 is the radius of the central path through the analyser and s is the size of the input (and output) apertures. For the CMA the resolving power is approximately $5.6R_1/s$ where R_1 is the radius of the inner cylinder and s is the size of the defining aperture; for the CMA this is not the size of the aperture in the inner cylinder (which is usually large) but of an aperture between the inner cylinder and the source and image points. Usually no real entrance aperture exists and so the source size determines the entrance aperture. In fact, the detailed design of a CMA is rather complex because the image aperture is not placed on the axis of the analyser; more detailed discussions of CMA design can be found in two general references on analyser design (Sevier, 1972; Roy & Carette, 1977).

Evidently these formulae for resolving power are sufficiently similar that the resolving powers of the two instruments are also similar for a comparable total analyser size. The geometry of the input acceptance angles, however, is quite different. The CMA is specifically designed to have a large acceptance angle; it may accept a range (~±6°) of incident angles about a mean of 42.3° to the axis,

at all azimuthal angles, leading to a total solid angle equal to almost 1 steradian. It has been used mostly for Auger electron spectroscopy, the effective entrance aperture being defined by the lateral dimensions of the incident electron beam used to excite the Auger electron emission (see section 2.3).

The CHA is traditionally fitted with a circular aperture subtending a total angle of less than 5° at the source, leading to an accepted solid angle of less than 10^{-2} steradians, ~100 times less than the CMA. However, the CHA is increasingly the instrument of choice in surface spectroscopy because it can be well matched to input lenses of circular symmetry (as shown schematically in Fig. 1.6) by allowing, for example, a larger working distance from the sample. These lenses can also be used to retard the electrons before they enter the analyser, effectively increasing the resolving power of the instrument by the retardation ratio (the incident energy divided by the energy at which the electrons pass through the analyser). The CHA is also ideally suited to the angle-resolved studies that are increasingly used in photoemission because of their increased information content (see sections 3.2.1, 5.1 and 6.2). Moreover, it has been shown to be well matched to parallel detection schemes if a two-dimensional position-sensitive detector is placed in the exit plane. For example, such a detector can measure (simultaneously) not only a small range of distinct energies displaced in the dispersion plane (the plane of the diagram) but also a range of detection angles of up to ~±12° perpendicular to this plane.

Of course, it is also possible to achieve the dispersion of energetic charged particles using magnetic, rather than electrostatic, fields but in the energy ranges relevant to surface techniques (mostly no more than a few keV) these are found to be less suitable. One alternative method of energy detection that is used, however, is to measure the time of flight (TOF) of the emitted particles over a well-defined pathlength. This approach has been most widely used for emitted ions (and neutral atoms), for which the flight times may be in the μs range. The TOF technique is potentially more challenging for the much lower-mass electrons, which have much shorter flight times for the same energy, although TOF detectors in photoemission are increasingly being explored. With sufficiently fast electronics and particle detectors this mode of energy detection can also achieve the independent detection of particles of many different energies with a single exciting pulse and thus it has the same advantage as that of parallel detection in an electrostatic dispersive analyser.

While the use of dispersive energy analysers is now the norm in almost all electron and ion detection experiments, it is appropriate to mention briefly the use of simple retarding field analysers (RFAs), which were first used for Auger electron spectroscopy (Chapter 2) and electron stimulated desorption (Chapter 6). The basic instrument is shown schematically in Fig. 1.7 and actually consists in this example of a standard LEED optics (see Chapter 3). Also shown is a typical energy spectrum of electrons emitted from a surface after impact by electrons of energy eV_E. The grid closest to the sample is set at the same potential as the sample

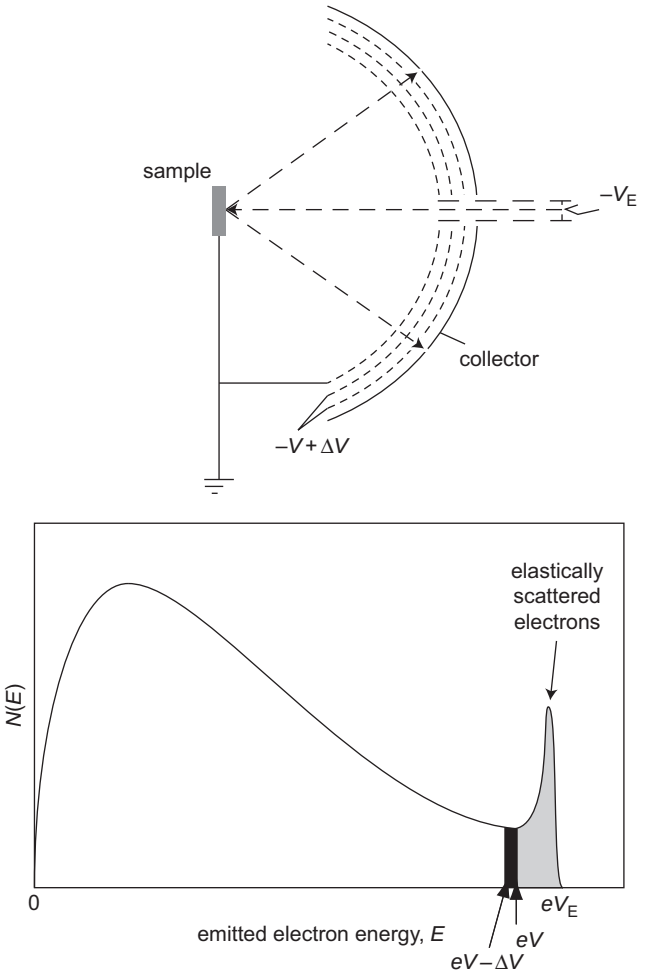

Fig. 1.7 (Upper) Schematic diagram of a LEED optics (see Chapter 3) operating as a simple retarding field electron energy analyser. (Lower) Scattered electron energy spectrum from incident electrons of energy eV_E showing (shaded) the electrons detected at the collector with a bias voltage V on the grids.

to ensure that the electrons travel in a field-free space. Applying a voltage $-V$ to the other grids then retards all electrons with an energy less than eV, while the higher energy electrons reach the collector. The device thus works as a high-pass energy filter, and the electrons that are collected correspond to the paler-shaded part of the energy spectrum in Fig. 1.7. If the grid voltage is changed to $V + \Delta V$, the current arriving at the collector is increased by the dark-shaded part of the energy spectrum. The difference between these two collector currents is thus equal to the number of emitted electrons in this narrow-ΔV energy window. Varying the retarding voltage thus provides access to the $N(E)$ spectrum, where $N(E)$ is

https://doi.org/10.1017/CBO9781139149716.004 Published online by Cambridge University Press

the number of electrons as a function of the energy E. The $N(E)$ spectrum can be measured directly by adding a small modulation voltage to V as it is scanned and detecting the in-phase harmonic part of the collected current. While clearly inferior to a truly dispersive electron energy analyser, the use of LEED optics in this way allowed early surface science researchers to move from a LEED-only instrument to one that could also detect Auger electron spectra at modest cost.

1.6 Surface Symmetry

The classification and description of the symmetry properties and structures of bulk (three-dimensional) crystalline materials requires a reasonable understanding of crystallography. Key issues are the restricted number of types of translational symmetry that crystals can possess (characterised by their associated unit cell, which must be one of the 14 Bravais lattices) and the finite number of point and space groups which can define the additional symmetry properties of all possible crystals. Many properties of solids are intimately related to the special symmetry properties of these materials. While a solid surface is intrinsically an imperfection of a crystalline solid, destroying the three-dimensional periodicity of the structure, this region of the solid retains two-dimensional periodicity (parallel to the surface), and this periodicity is an important factor in determining some properties of the surface. In particular, it plays a dominant role in allowing electron, X-ray and atom diffraction techniques to provide information on the structure of the surface as well as strongly influencing the electronic properties of the surface. For these reasons a proper understanding of surface crystallography is important for a general understanding of many surface effects and is critical for an understanding of the electron, X-ray and atom diffraction techniques discussed in Chapter 3.

In discussing the structure of solid surfaces it is helpful to develop a notation which minimises confusion. A surface, in the mathematical sense, cannot have structure so by 'surface structure' is meant the structure of the solid in the vicinity of the surface. For this reason it is useful to define a region of chemically pure solid in the vicinity of the mathematical surface as the *selvedge* (by analogy with the edge of a piece of cloth). The sample to be studied can then be thought of as a *substrate*, which has the proper three-dimensional periodicity of the bulk plus the few atomic layers of the selvedge, which may adopt atomic sites different from those of the underlying bulk (Fig. 1.8). For example, it is probable that the layer spacing normal to the surface will differ slightly from that of the bulk (substrate). It is also possible that reconstruction may take place involving atom movements parallel to the surface in the selvedge (as is known to happen, for example, for some surfaces of Si, Ge, Au and Pt in their 'clean' condition). The selvedge, however, is crystalline in the sense that it retains periodicity parallel to the surface; i.e. it is two-dimensionally periodic.

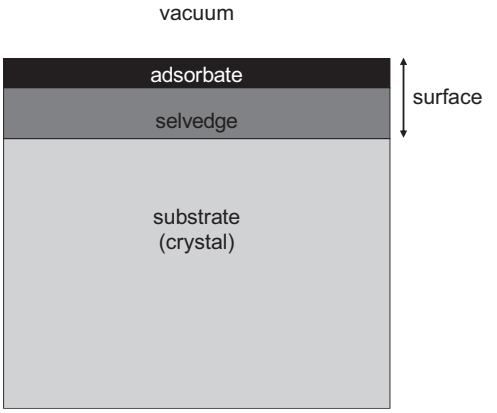

Fig. 1.8 Surface terminology. The 'surface' is the sum of the modified part of the crystalline substrate (the selvedge) and any outer atomic layer(s) containing atoms of molecules of different species (the adsorbate).

Evidently in reconstructed surfaces this lateral periodicity generally differs from that of the substrate, although it is usually commensurate with the substrate periodicity – i.e. both selvedge and substrate have a common periodicity that is greater than that of the substrate (and may be greater than either part in isolation). This terminology really only covers clean surfaces. Often the surface structure of interest involves an *adsorbate*, commonly comprising atoms or molecules that have come from the surrounding gas phase, although they may also have *segregated* from the underlying bulk. More generally, therefore, what is meant by the properties of the surface is the properties of the selvedge plus, if present, any adsorbate. Notice that the introduction of an adsorbate may well change the structure of the selvedge, and indeed the adsorbate may penetrate into the selvedge.

It is the two-dimensional periodicity of the surface that enables us to classify the possible symmetry elements and symmetrically different surface structures. It is helpful, however, to clarify the formal reasons for, and extent of, the loss of periodicity in the third dimension. Any surface technique, by definition, penetrates only a small way into the solid. The signal that emerges is likely to contain a large contribution from the top atom layer, a weaker contribution from the next layer, and so on. The effective depth of penetration varies from technique to technique and is a function of the particular conditions of the experiment. Most techniques, however, penetrate deep enough into the material to contain significant contributions from adsorbate (if present), selvedge and substrate. Thus, from the point of view of classifying the two-dimensional symmetry properties (i.e. those symmetries involving only operations within planes parallel to the surface), it is generally necessary to consider symmetries that are properties of the whole adsorbate, selvedge and substrate complex, and not simply of

one component or one layer of this whole. The symmetries operate in two dimensions but the surface structure is entirely three-dimensional. In some special cases it is possible that the penetration of a surface probe is shallow enough for higher symmetries to be observed because only a small part of this complex is 'seen' by the technique. Of course, even if the whole surface region of the crystal has the same atomic structure as that of the substrate (i.e. there is effectively no adsorbate or selvedge), the technique, by virtue of its surface specificity, 'sees' only a two-dimensionally periodic system; successive atom layers become inequivalent by virtue of the limited penetration itself.

In addition to the translational symmetry parallel to the surface that characterises its crystallinity, the surface may possess a small number of point and line symmetry operations that involve rotation or reflection within planes parallel to the surface. This whole subject is dealt with in many undergraduate solid state physics textbooks and is fully classified in detail in the *International Tables for X-ray Crystallography* (1952). Briefly, these symmetry operations are (the trivial) one-fold rotation, rotations about two-, three-, four- and six-fold rotation axes, mirror reflection in a plane perpendicular to the surface and glide reflection (meaning reflection in a line combined with translation along the direction of the line by half the translational periodicity in this direction). Note that a five-fold or more than six-fold rotation axis is not compatible with the two-dimensional translational symmetry. Consideration of the symmetry properties of two-dimensional lattices (nets or meshes) leads to just five symmetrically different Bravais nets. These are: hexagonal, characterised by a six-fold rotation axis: square, characterised by a four-fold rotation axis; primitive or centred rectangular, corresponding to the *two* symmetrically non-equivalent lattices characterised by mirror symmetry; and oblique, which lacks all these symmetries. Note that the centred rectangular net is the only non-primitive net. The centring of any other net leads only to nets that can be equally well classified by primitive nets of the same symmetry. Combining these five Bravais nets with the ten different possible point groups leads to just 17 possible two-dimensional space groups. There are thus only 17 possible symmetrically different types of surface structure (although, of course, there is an infinite number of possible surface structures). These nets, point groups and space groups are shown in Figs. 1.9, 1.10 and 1.11 and Table 1.3.

It is worth noting that even in the case of an unreconstructed clean surface the surface unit net is not necessarily a simple projection of the three-dimensional unit cell onto the surface plane. Consider, for example, the {100} surface (i.e. a plane surface parallel to the {100} set of planes) of a face-centred cubic (fcc) solid. Figure 1.12 shows schematically a view looking down onto such a surface (i.e. a projection of the solid onto the surface). This surface has square symmetry as expected, because both the 'surface' and bulk have four-fold rotation axes

Table 1.3 *The five two-dimensional Bravais nets*

Shape of unit mesh	Mesh symbol	Conventional rule for choice of axes	Nature of axes and angles	Name
General parallelogram	p	None	$a \neq b$ $\gamma \neq 90°$	Oblique
Rectangle	p c	Two shortest mutually perpendicular vectors	$a \neq b$ $\gamma = 90°$	Rectangular
Square	p	Two shortest mutually perpendicular vectors	$a = b$ $\gamma = 90°$	Square
60° angle rhombus	p	Two shortest vectors at 120° to each other	$a = b$ $\gamma = 120°$	Hexagonal

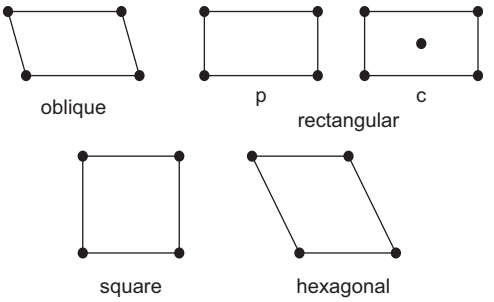

Fig. 1.9 The five two-dimensional Bravais nets: the specifications are given in Table 1.3.

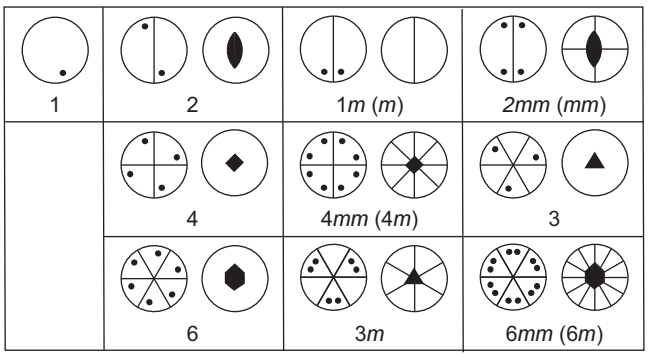

Fig. 1.10 Stereograms of the ten two-dimensional point groups. On the left of each panel is shown the equivalent positions and on the right the symmetry operations. The names follow the full and (in parentheses) abbreviated 'International' notation.

https://doi.org/10.1017/CBO9781139149716.004 Published online by Cambridge University Press

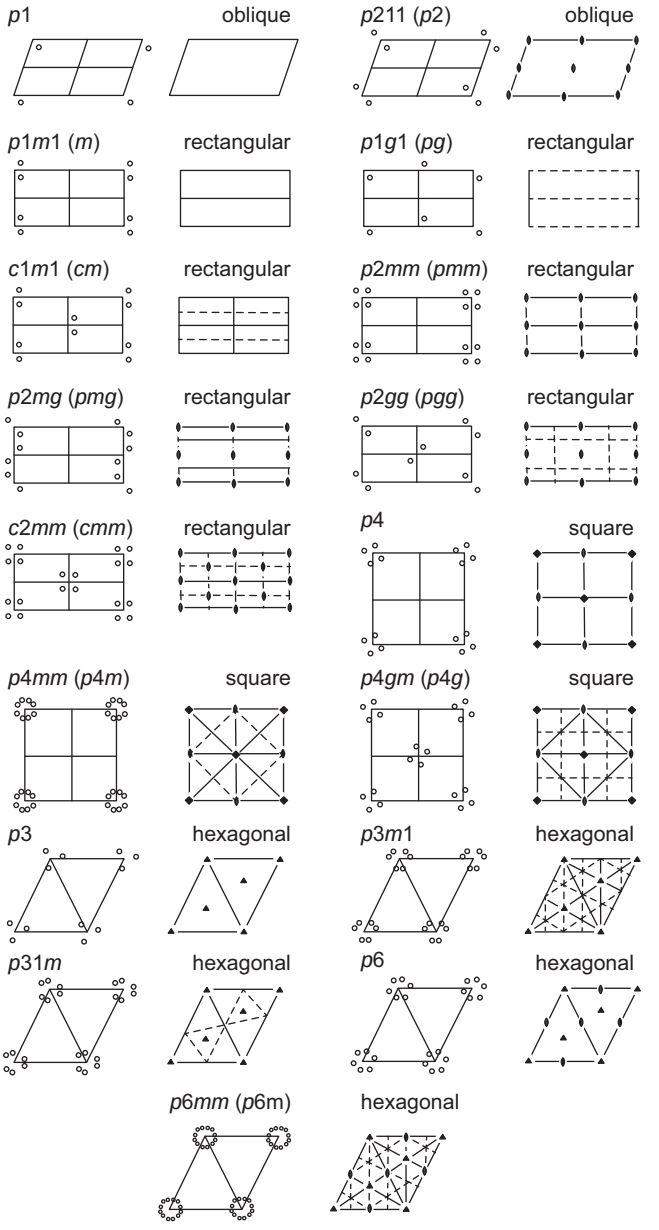

Fig. 1.11 Equivalent positions, symmetry operations and long and short 'International' notations for the 17 two-dimensional space groups.

perpendicular to this surface. However, the surface Bravais net is described by the primitive square unit mesh shown in solid lines on the right of Fig. 1.12. The end or projection of a three-dimensional face-centred unit cell, shown on the left by broken lines, forms a centred square unit mesh with twice the area of the true unit mesh. As

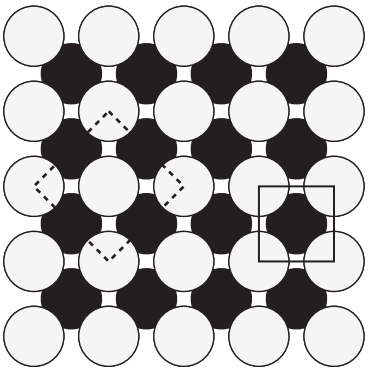

Fig. 1.12 Schematic plan view of a {100} surface of an fcc solid with the top-layer (and odd-numbered-layer) atoms shown as light-shaded circles, and the second-layer (and even-numbered-layer) atoms shown as dark-shaded circles. The unit net shown with broken lines on the left is the projection of the three-dimensional (non-primitive) unit cell. On the right the solid lines indicate the primitive surface unit net.

explained above, a centred square mesh is symmetrically identical to a primitive square net and this is therefore an inappropriate description. This kind of difference in description using a two-dimensional mesh and a three-dimensional unit cell arises, of course, because of the use of a non-primitive unit cell in three dimensions (which *is* a symmetrically distinct three-dimensional Bravais lattice), but this can lead to confusions of notation, particularly in reciprocal space (see section 3.1).

1.7 Description of Overlayer Structures

If the surface layers of a solid differ structurally from the substrate, owing to a reconstructed selvedge or because of the presence of an adsorbate or both of these, then the structure within these layers may be either disordered, ordered and commensurate with the substrate, or ordered and incommensurate with the surface. Evidently the first case is of little interest from the point of view of surface crystallography. Provided order does exist in the adsorbate or selvedge, however, it is convenient to describe this order by relating its Bravais net to that of the underlying substrate. This is usually done in one of two ways, the most general of which, proposed by Park & Madden (1968), involves a simple vectorial construction. If the primitive translation vectors of the substrate unit net are $\mathbf{a}$ and $\mathbf{b}$ and those of the adsorbate and/or selvedge are $\mathbf{a}$ and $\mathbf{b}'$ then their relationship can be written as

$$\mathbf{a}' = G_{11}\mathbf{a} + G_{12}\mathbf{b} \tag{1.7}$$

$$\mathbf{b}' = G_{21}\mathbf{a} + G_{22}\mathbf{b} \tag{1.8}$$

where the G_{ij} are four coefficients which form a matrix G,

$$G = \begin{pmatrix} G_{11} & G_{12} \\ G_{21} & G_{22} \end{pmatrix} \tag{1.9}$$

such that the absorbate plus selvedge and substrate meshes are related by

$$\begin{pmatrix} \mathbf{a}' \\ \mathbf{b}' \end{pmatrix} = G \begin{pmatrix} \mathbf{a} \\ \mathbf{b} \end{pmatrix} \tag{1.10}$$

Another property of this matrix is that, because the area of the substrate unit mesh is given by $|\mathbf{a} \times \mathbf{b}|$, the determinant of G, det G, is simply the ratio of the areas of the two meshes and provides a convenient classification system for the type of surface structure involved, as follows:

(a) det G *is integral and all matrix components are integral* The two meshes are simply related. The adsorbate plus selvedge mesh has the same translational symmetry as the whole surface.

(b) det G *is a rational fraction (or* det G *is integral and some matrix components are rational)* The two meshes are rationally related. In this case the structure is still commensurate but the true surface mesh is larger than either the substrate or adsorbate plus selvedge mesh. This surface mesh has a size dictated by the distances over which the two meshes come into coincidence at regular intervals, and for this reason such structures are frequently referred to as *coincidence lattice* (or more properly *coincidence net)* structures. The true surface mesh now has primitive translation vectors $\mathbf{a}''$ and $\mathbf{b}''$, which are related to the substrate and adsorbate meshes by matrices P and Q such that

$$\begin{pmatrix} \mathbf{a}'' \\ \mathbf{b}'' \end{pmatrix} = P \begin{pmatrix} \mathbf{a} \\ \mathbf{b} \end{pmatrix} = Q \begin{pmatrix} \mathbf{a}' \\ \mathbf{b}' \end{pmatrix} \tag{1.11}$$

det P and det Q being chosen to have the smallest possible integral values. They are related by

$$\det G = \frac{\det P}{\det Q} \tag{1.12}$$

(c) det G is *irrational* The two meshes are now incommensurate and no true surface mesh exists. Such a situation implies that the substrate is simply providing a flat surface on which the adsorbate or selvedge can form its own two-dimensional structure. This might be expected, for example, if adsorbate–adsorbate bonding is very much stronger than the lateral corrugation of the adsorbate–substrate potential.

A somewhat more convenient, but less versatile, notation for surface mesh structures that is widely used is that suggested by Wood (1964). In this case the notation

defines the ratio of the lengths of the surface and substrate meshes, together with the angle through which one mesh must be rotated to align the two pairs of primitive translation vectors. In this notation, if adsorbate A on the $\{hkl\}$ surface of material X causes the formation of a structure having primitive translation vectors of length $|\mathbf{a}'| = p|\mathbf{a}|$ and $|\mathbf{b}'| = q|\mathbf{b}|$ and a unit mesh rotation ϕ then the structure is referred to as

$$\mathrm{X}\{hkl\}p \times q - R\phi - \mathrm{A}$$

or often

$$\mathrm{X}\{hkl\}(p \times q)R\phi - \mathrm{A}$$

Note that this notation can only be used if the included angles of the surface and substrate unit meshes are the same. Thus, while it is suitable for systems where the surface and substrate meshes have the same Bravais net or where one mesh is rectangular and the other square, in general it is not adequate to describe mixed symmetry meshes. An extension of the Wood notation, which seems to have been first used by Biberian & Van Hove (1984), can be used to describe the case of a rectangular unit mesh on a hexagonal substrate. In this case, if the dimensions of the rectangular mesh are specified by the length ratios p and q, then $R\phi^\circ$ is replaced by 'rect.' (see Fig. 1.13 for an example of such meshes). In all other cases the matrix notation must be used. As examples of the Wood notation, a clean unreconstructed Ni{100} surface is denoted by Ni{100}(1×1) while one structure formed by the adsorption of O on this surface is the Ni{100}(2×2)–O structure. By contrast, the Si{100} surface is typically reconstructed to Si{100}(2×1) in its clean state, but the adsorption of atomic H can 'unreconstruct' the surface to give Si{100}(1×1)–H. Some examples of surface nets and their matrix and Wood notations are given in Fig. 1.13. One particular example of note, in Fig. 1.12(b), is the $(\sqrt{2}\times\sqrt{2})R45^\circ$ structure on the square mesh, which commonly occurs on cubic {100} surfaces. It is most often referred to in terms of a centred unit mesh, $\sqrt{2}$ times larger and not rotated relative to the substrate mesh, as c(2×2), thus encouraging the use of the notation p(2×2) for a true (2×2) structure. As shown above, no centred square Bravais net exists as a symmetrically distinct mesh from the primitive square mesh, so this nomenclature is crystallographically incorrect but it is so widely used that it has effectively become absorbed into the nomenclature.

1.8 Theoretical Studies of Surfaces

This book is concerned with techniques for experimental studies of surfaces, but as in any area of science, complementary theoretical studies play an important role. Of course, extracting information from experimental methods generally involves

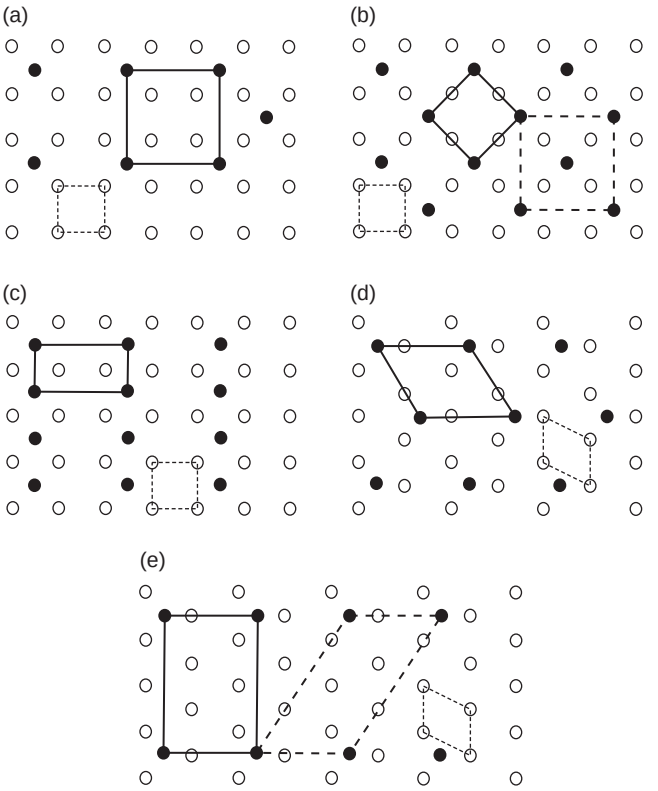

Fig. 1.13 Examples of some simply related surface meshes and their notation. In each figure the open circles represent the substrate periodicity and the filled circles the surface periodicity. In all cases the short-broken lines show the substrate unit net while the solid lines define a surface unit net. In (a) the square surface unit net is defined in the matrix notation by $\begin{bmatrix} 2 & 0 \\ 0 & 2 \end{bmatrix}$ and in the Wood notation by (2×2), while in (b) the surface unit net is $\begin{bmatrix} 1 & \bar{1} \\ 1 & 1 \end{bmatrix}$ or $(\sqrt{2}\times\sqrt{2})R45°$, although this is also often described by the unit net shown by long-broken lines as c(2×2). Panel (c) shows a case of a rectangular surface mesh on a square substrate described as $\begin{bmatrix} 2 & 0 \\ 0 & 1 \end{bmatrix}$ or (2×1). Panels (d) and (e) show examples of structures on a hexagonal substrate. Note that in standard crystallographic convention (Table 1.3) the primitive translation vectors are defined as separated by 120° (not 60°). The surface unit net in (d) is thus $\begin{bmatrix} 2 & 1 \\ \bar{1} & 1 \end{bmatrix}$ or $(\sqrt{3}\times\sqrt{3})R30°$. In (e) the rectangular surface unit net is $\begin{bmatrix} 2 & 1 \\ 0 & 3 \end{bmatrix}$ or in the extended Wood notation $(\sqrt{3}\times 3)$rect. An alternative description in the standard Wood notation, based on the long-broken unit net, is $(\sqrt{3}\times 2\sqrt{3})R30°$.

https://doi.org/10.1017/CBO9781139149716.004 Published online by Cambridge University Press

some theoretical calculations based on the physical principles of the method but in surface science, as in a range of investigations of molecules and materials (including biological materials), an increasingly important role is played by total energy calculations based, in particular, on density functional theory (DFT). The development of these methods, in parallel with the huge advances in computational resources, means that the total electronic energy of a system can be explored as a function of its structure, which is then adjusted until the most favourable, lowest-energy, structure is found. The results of such a calculation provide not only a theoretical determination of the optimum geometry but also details of the electronic structure.

The remarkable success of DFT calculations applied to surfaces in the last few years has meant that in some cases (for example in some catalyst design work) these methods are used to replace experiments. Despite their power, however, there are sufficient examples of disagreement between experiment and theory to show that such a high level of faith in the methods in all cases may be misplaced. It is also important to recognise that identifying the minimum energy structure involves the same underlying problems as determining a surface structure experimentally. Specifically, essentially all these techniques exploit a 'trial-and-error' approach, described in Chapter 3, in which the results of an experimental simulation for a model (trial) structure are compared with those of the actual experiment; the structural parameters of the model are then modified until one achieves good agreement with experiment. This process can only identify the correct structure if the correct basic model is tested, and the same limitation applies to DFT determinations of the minimum energy structure. The search algorithms used to find the minimum energy allow atom movements but do not, for example, allow the addition or removal of atoms that may arise in a surface reconstruction.

Despite these caveats, there is no doubt that the complementary use of DFT calculations and experiments has proved to be a powerful combination in surface science. One obvious example is in STM investigations of surface structures. As described in Chapter 4, while STM provides sub-atomic images of surfaces, the fact that it really probes the spatial variation of the electronic structure of the surface means that the interpretation of these images in terms of atomic positions is far from trivial. Calculations using DFT can provide a basis for simulations of STM images within a simplified model that can allow a substantial improvement in the most probable structural interpretation of these data. Further discussion of DFT methods and their application is beyond the scope of the present book but can be found, for example, in the books by Sholl & Steckel (2009) and Engel & Dreizler (2011).